Supplementary information

1 ECM turnover model

We explore the impact of including a general saturating ECM production term, which is dependent on the normal cells, by extending the model as follows:

$$\frac{\partial \eta_1}{\partial \tau} = \eta_1(1-\eta_1) - \gamma_1 \Lambda \eta_1 \tag{1}$$

$$\frac{\partial \eta_2}{\partial \tau} = \delta_2 \eta_2(1-\eta_2) + \nabla_\xi \cdot [\alpha_2(1-\eta_1)(1-\eta_3)\nabla_\xi \eta_2] \tag{2}$$

$$\frac{\partial \Lambda}{\partial \tau} = \delta_3(\eta_2 - \Lambda) + \nabla_\xi^2 \Lambda \tag{3}$$

$$\frac{\partial \eta_3}{\partial \tau} = \delta_4 \eta_1 \eta_3(1-\eta_3) - \Gamma \eta_3 \tag{4}$$

$$\frac{\partial \Gamma}{\partial \tau} = \delta_5 \eta_1 \eta_2 - \gamma_5 \Gamma + \alpha_5 \nabla_\xi^2 \Gamma \tag{5}$$

where $\delta_4 = \frac{r_4 K_1}{r_1}$.

Here we include a saturating ECM production term in Equation (4), which is dependent on the presence of normal cells. The rate of ECM production is given by the parameter δ_1.

Figure 3 shows the percent reduction in wavespeed for a range of values of ECM production, δ_1, and selected tumour aggression values of γ_1. As expected, increasing the ECM production rate decreases the wavespeed for a given γ_1, as the production of ECM negates any degradation by the activated MMPs. Increasing ECM turnover by several orders of magnitude can result in reductions of wavespeed by 50-80%. Nevertheless, the presence of ECM turnover is not enough to halt invasion within the wide range of parameter values examined. Furthermore, if the tumour cells rely on matrix remodelling (instead of degradation), the reductions in wavespeed seen in Figure 3 would be even less, as it is unlikely that cellular

elements would produce ECM in the presence of ECM which has only been remodelled.

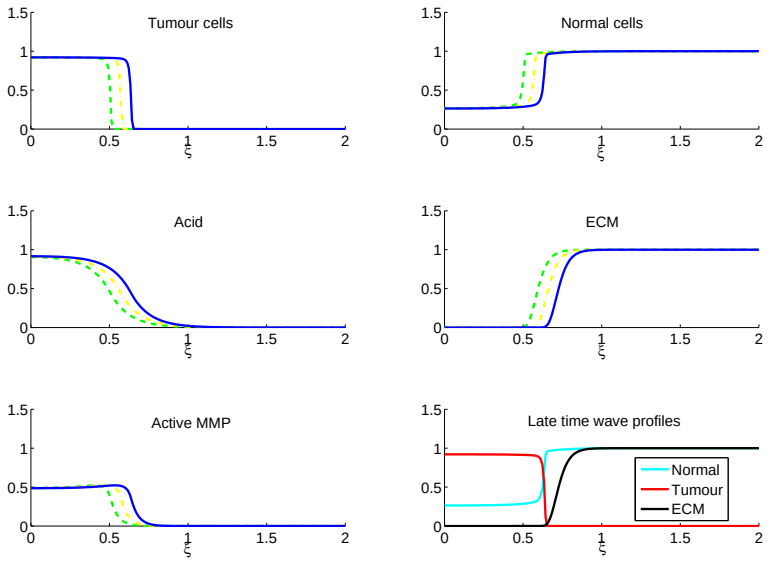

Figure 1: In colour online. Tumour cell, normal cell, acid, ECM, and MMP profiles through time of Equations (16)-(20) with direct competition ($\beta_1 = 0.7$ and $\beta_2 = 0.3$). Here, $\gamma_1 = 0.5$ and the profiles are shown with $\tau = 160$ (green dash), $\tau = 180$ (yellow dash-dot), and $\tau = 200$ (blue line). The lower right figure shows the late time ($\tau = 200$) profiles of the normal tissue (cyan), tumour tissue (red), and ECM (black). In these simulations, total cell density behind the advancing tumour front is reduced compared to the case where $\beta_1 = \beta_2 = 0$. The system is solved with parameters as in Table 1, initial conditions as in Equations (11)-(15), boundary conditions as detailed in the text, with the simulations run up to $\tau = 200$.

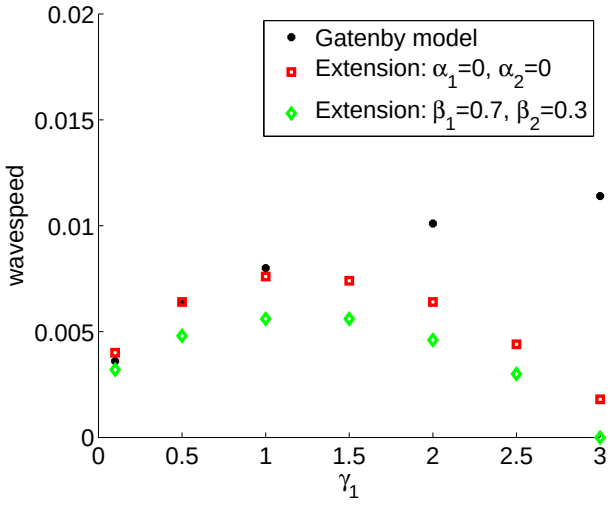

Figure 2: In colour online. Numerically calculated late time tumour invasion speed with the Gatenby-Gawlinski model (black circles) *versus* extended model without competition (red squares, solutions to Equations (6)-(10)) *versus* extended model with competition (green diamonds, solutions to Equations (16)-(20), $\beta_1 = 0.7$ and $\beta_2 = 0.3$) with varying γ_1. The inclusion of competition reduces the wavespeed for low γ_1 due to less total cell density and MMP production, but the qualitative results are similar compared to the no competition model. The system is solved with parameters as in Table 1, initial conditions are used as in Equations (11)-(15), boundary conditions are as detailed in the text, with the simulations run up to $\tau = 200$. The late time invasion speed is calculated from the speed of the tumour front (designated at $\eta_1 = 0.5$, and located via interpolation) during the last $\Delta\tau = 5$ interval.

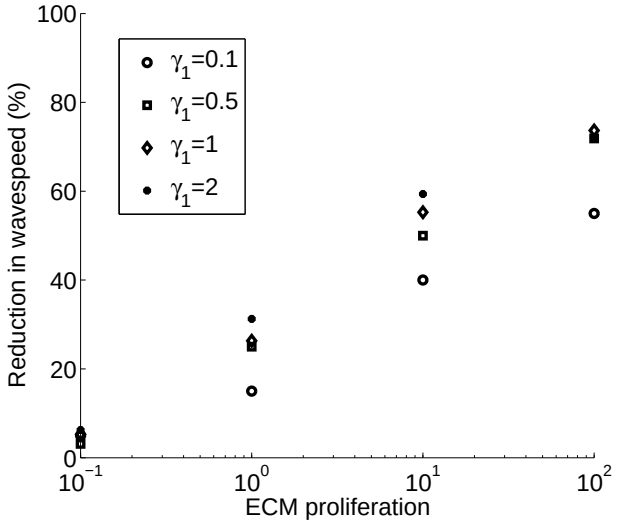

Figure 3: The reduction in wavespeed (vertical axis) found with various levels of ECM turnover (horizontal axis) and at several values of tumour aggression, γ_1 (as noted in legend). Low rates of ECM turnover result in little deviation from results with no turnover. However, at very high rates of turnover (δ_4 ten times that of the tumour proliferation parameter, δ_2) reductions of 40-60% can be seen. The system (Supplementary Equations (1)-(5)) is solved with parameters as in Table 1 and δ_5 as noted in the figure, initial conditions as in Equations (11)-(15), boundary conditions as detailed in the text, with the simulations run up to $\tau = 200$.